European Heart Journal Advance Access published July 2, 2010

European Heart Journal
doi:10.1093/eurheartj/ehq237

FASTTRACK

Arterial and aortic valve calcification inversely correlates with osteoporotic bone remodelling: a role for inflammation

Jesper Hjortnaes[1†], Jonathan Butcher[2,3†], Jose-Luiz Figueiredo[1,4], Mark Riccio[3], Rainer H. Kohler[1], Kenneth M. Kozloff[5], Ralph Weissleder[1], and Elena Aikawa[1,4*]

[1]Center for Molecular Imaging Research, Massachusetts General Hospital, Boston, MA, USA; [2]Department of Biomedical Engineering, Cornell University, Ithaca, NY, USA; [3]Preclinical Imaging Facility, Cornell University, Ithaca, NY, USA; [4]Brigham and Women's Hospital, Harvard Medical School, 77 Avenue Louis Pasteur, NRB7, Boston, MA 02115, USA; and [5]Department of Orthopaedic Surgery, University of Michigan, Ann Arbor, MI, USA

Received 18 May 2010; revised 16 June 2010; accepted 25 June 2010

Aims Westernized countries face a growing burden of cardiovascular calcification and osteoporosis. Despite its vast clinical significance, the precise nature of this reciprocal relationship remains obscure. We hypothesize that cardiovascular calcification progresses with inflammation and inversely correlates with bone tissue mineral density (TMD).

Methods and results Arterial, valvular, and bone metabolism were visualized using near-infrared fluorescence (NIRF) molecular imaging agents, targeting macrophages and osteogenesis. We detected significant arterial and aortic valve calcification in apoE$^{-/-}$ mice with or without chronic renal disease (CRD, 30 weeks old; $n = 28$), correlating with the severity of atherosclerosis. We demonstrated decreases in osteogenic activity in the femurs of apoE$^{-/-}$ mice when compared with WT mice, which was further reduced with CRD. Three-dimensional micro-computed tomography imaging of the cortical and cancellous regions of femurs quantified structural remodelling and reductions in TMD in apoE$^{-/-}$ and CRD apoE$^{-/-}$ mice. We established significant correlations between arterial and valvular calcification and loss of TMD ($R^2 = 0.67$ and 0.71, respectively). Finally, we performed macrophage-targeted molecular imaging to explore a link between inflammation and osteoporosis *in vivo*. Although macrophage burden, visualized as uptake of NIRF-conjugated iron nanoparticles, was directly related to the degree of arterial and valvular inflammation and calcification, the same method inversely correlated inflammation with TMD ($R^2 = 0.73$; 0.83; 0.75, respectively).

Conclusion This study provides direct *in vivo* evidence that in arteries and aortic valves, macrophage burden and calcification associate with each other, whereas inflammation inversely correlates with bone mineralization. Thus, understanding inflammatory signalling mechanisms may offer insight into selective abrogation of divergent calcific phenomena.

Keywords Aortic valve calcification • Atherosclerosis • Inflammation • Bone mineral density • Molecular imaging

Introduction

Clinical studies suggest that cardiovascular calcification, atherosclerosis, and chronic renal disease (CRD) are associated with osteoporosis.[1,2] Emerging epidemiological evidence shows age-independent correlation between bone mineral density and cardiovascular events.[3–5] In limited mouse studies, atherosclerosis susceptibility corresponds to a reduction in bone mineralization.[6,7] Although these observations suggest common underlying mechanisms, the precise nature of the relationship between arterial calcification, calcific aortic valve disease, and bone osteogenesis, as well as reciprocal regulation of these processes, remains unknown. The National Heart, Lung, and Blood Institute Working Group on Calcific Aortic Stenosis has recently

† The first two authors contributed equally to the study.

* Corresponding author. Tel: +1 617 730 7755, fax: +1 617 730 7791, Email: eaikawa@partners.org; eaikawa@rics.bwh.harvard.edu

underscored the importance of identifying the relationship between calcification of the aortic valve and bone and the reciprocal regulation of these processes.[8]

Arterial and aortic valve calcification is a significant cause of morbidity and mortality.[9,10] Arterial calcification not only weakens vasomotor responses, but also affects atherosclerotic plaque stability. Emerging evidence suggests that atherosclerotic plaques are prone to rupture, particularly in regions of high background stress with microcalcifications located in the thin fibrous cap.[11–13] In addition, calcification impairs the movement of aortic valve leaflets, causing life-threatening aortic stenosis and heart failure.[14] Recent studies suggest that underlying mechanisms of aortic valve calcification resemble those of atherosclerotic arterial calcification, triggered by haemodynamic stress, reactive oxygen species, and inflammatory cues.[14–17]

Cardiovascular calcification was conventionally viewed as an inevitable consequence of ageing, but recent landmark studies have demonstrated that it is a highly regulated process of mineralization, akin to embryonic bone formation.[14,18] Indeed, calcified vascular material is often indistinguishable from bone, and its formation involves cellular and molecular signalling processes found in normal osteogenesis.[19,20] We have reported that valvular myofibroblast-like cells, due to their plasticity, respond to various stimuli by undergoing activation and sequential phenotypic differentiation. During cardiovascular calcification, macrophage-derived proteinases such as elastolytic cathepsins or metalloproteinases induce the release of biologically active, soluble elastin-derived peptides that may promote the osteogenic differentiation of myofibroblasts or smooth muscle cells (SMC).[21] This finding concurs with studies of phenotypic conversion of vascular SMC and valvular myofibroblasts into osteoblastic cells, characterized by the expression of bone-regulating proteins and osteogenic factors (e.g. alkaline phosphatase, osteopontin, osteocalcin, Runx2/Cbfa1, Osterix).[16,22,23]

Imaging approaches that can spatially resolve and quantify the temporal pro-osteogenic molecular processes in arteries, valves, and bones are limited. Conventional imaging modalities can identify advanced late-stage calcification, but optical molecular imaging can detect tissue mineralization at the earliest stages. The present study tested the hypothesis that arterial and aortic valve calcification is inversely correlated with low bone tissue mineral density (TMD). The specific objective was to quantify the relationship between cardiovascular calcification (arterial and valvular) and long bone remodelling (cortical and trabecular) in established models of atherosclerosis and CRD,[14–16] using optical molecular imaging and high-resolution 3D micro-computed tomography (CT). In addition, to demonstrate the association between inflammation, ectopic calcification, and osteoporosis, we directly compared macrophage burden and progression of osteogenic changes in each region of the same animals *in vivo* and *ex vivo*. Our results on opposing effects of inflammation in soft tissues (cardiovascular organs) and in bone agree with the previous reports on accelerated osteolysis in inflamed bones.[24] Our study provides new insight into the relationship between osteoporosis and cardiovascular calcification and suggests shared inflammatory mechanisms of ectopic calcification and bone osteolysis. It also offers a unique model for exploration of *in vivo* mechanisms regulating early cardiovascular calcification and bone mineral loss.

Methods

An expanded Methods section is provided in the Supplementary material online.

Animal protocol

We studied osteogenic changes in carotid arteries, aortic valves, and femur bones obtained from 30-week-old apoE$^{-/-}$ mice ($n = 10$) and mice with CRD ($n = 10$), induced by 5/6 nephrectomy. Age-matched wild-type C57/BL6 mice (WT, $n = 8$) served as controls. At 30 weeks of age, mice underwent intravital microscopy and were euthanized for *ex vivo* imaging, followed by histology and statistical analyses. In addition to molecular imaging, the femurs of the mice underwent quantitative micro-CT imaging analyses. The Subcommittee on Research Animal Care at Massachusetts General Hospital approved all procedures.

Molecular imaging agents

To image osteogenesis, we used imaging agent (Osteosense680/OS680, VisEn Medical, Inc., Woburn, MA, USA) binding to hydroxyapatite in actively mineralized regions containing osteoblast-like cells in arteries, valves[14–16] (Supplementary material online, *Figure S1A*), and bones.[25] Macrophage-targeted near-infrared (NIR)-conjugated iron nanoparticle (Supplementary material online, *Figure S1B*) was used to detect inflammation.[14–16]

Statistical analyses

Data are presented as mean ± standard deviation. Statistical analyses for comparison groups employed one-way ANOVA, followed by the Tukey–Kramer *post hoc* test performed with GraphPad prism software (version 4.0, GraphPad Software, San Diego, CA, USA). Tests were two-sided and adjusted for variance inequality where appropriate. Linear regression with Pearson's correlation test was used to determine the covariant relationships between data. Normal distribution of the data was confirmed by comparing against expected normal distributions with given means and standard deviation. In all cases, test probability values less than 0.05 were considered statistically significant.

Results

Serum phosphate, creatinine, cystatin C, and cholesterol levels in apoE$^{-/-}$ and chronic renal disease apoE$^{-/-}$ mice

Total cholesterol was significantly increased in apoE$^{-/-}$ and CRD apoE$^{-/-}$ mice, when compared with WT mice (467.2 ± 51.1 and 397.1 ± 24.8 mg/dL vs. 56.3 ± 9.8 mg/dL; $P < 0.05$). In addition, CRD apoE$^{-/-}$ mice had significantly increased serum phosphate, creatinine, and cystatin C levels when compared with apoE$^{-/-}$ and WT mice (phosphate: 11.4 ± 0.9 vs. 6.3 ± 0.4 and 4.7 ± 0.4 mg/dL; $P < 0.05$; creatinine: 0.6 ± 0.04 vs. 0.4 ± 0.01 and 0.3 ± 0.01 mg/dL; $P < 0.05$; cystatin C: 0.9 ± 0.01 vs. 0.6 ± 0.2 and 0.3 ± 0.02 μg/mL; $P < 0.001$). Greater serum phosphate, creatinine, and cystatin C levels suggest that 5/6 nephrectomy induced kidney failure, which in turn promotes inflammation.[15]

Osteogenic activity in mouse arteries and aortic valves associate with each other and increase with atherosclerosis severity

Fluorescence reflectance imaging was used to map mineralization in aortas of WT, apoE$^{-/-}$, and CRD apoE$^{-/-}$ mice. Strong signals were detected at the levels of aortic valve, aortic root, aortic arch, and abdominal aorta, in apoE$^{-/-}$ and especially CRD apoE$^{-/-}$ mice when compared with WT mice (Supplementary material online, *Figure S2*). Intravital imaging of carotid arteries *in vivo* showed more than 47- and 78-fold increases of calcified tissue area (ROI) in apoE$^{-/-}$ and CRD apoE$^{-/-}$ mice, respectively, compared with WT cohort (*Figure 1A* and *B*). In addition, up to 100- and 400-fold increases in osteogenic signal intensity (SI) occurred in apoE$^{-/-}$ and CRD apoE$^{-/-}$ mice, respectively, when compared with the WT cohort (*Figure 1A* and *C*). Imaging analyses of the aortic valves in WT, apoE$^{-/-}$, and CRD apoE$^{-/-}$ mice revealed that ROI increased 4- and 20-fold in size in apoE$-/-$ and CRD apoE$^{-/-}$ mice, respectively, compared with ROI in WT mice (*Figure 1D* and *E*). Osteogenic SI was further significantly increased in aortic valves of apoE$^{-/-}$ and CRD apoE$^{-/-}$ mice (13- and 50-fold, respectively) when compared with WT mice (*Figure 1D* and *F*). We performed a correlative analysis, in addition to Pearson's correlation test, to evaluate an association between vascular and valvular calcification. *Figure 1G* shows a significant correlation of arterial and aortic valve calcific ROI ($r = 0.75$; $P < 0.05$). In addition, arterial osteogenic SI significantly correlated with valvular SI ($r = 0.67$; $P < 0.05$; *Figure 1H*).

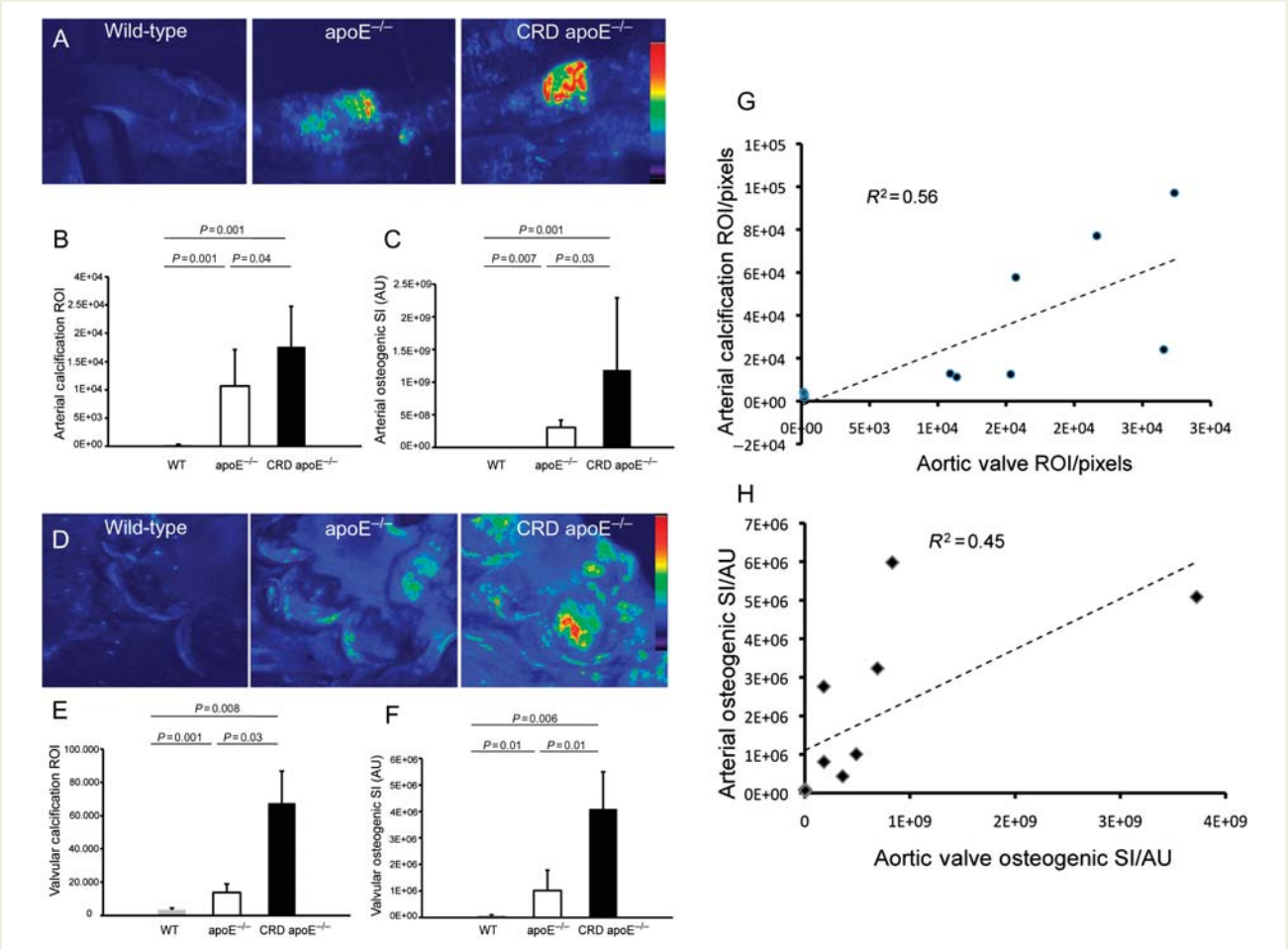

Figure 1 Induction of osteogenesis in carotid arteries and aortic valves of apoE$^{-/-}$ and chronic renal disease apoE$^{-/-}$ mice, detected by intravital fluorescence microscopy. (*A*) Calcified regions (region of interest) and mineralization (signal intensities) in the carotid arteries of WT, apoE$^{-/-}$, and chronic renal disease apoE$^{-/-}$ mice injected with Osteosense680 (maximum signal intensity shown in red). (*B*) Quantitative assessment of region of interest showed a significant increase in calcification in the chronic renal disease apoE$^{-/-}$ vs. WT and apoE$^{-/-}$ mice. (*C*) Arterial osteogenic signal intensity is greater in the chronic renal disease apoE$^{-/-}$ mice, compared with other groups. (*D*) Pseudo-colour mapping of mineralization region of interest and signal intensity in the aortic valves. Aortic valve calcified region of interest (*E*) and osteogenic signal intensity (*F*) are significantly higher in the chronic renal disease apoE$^{-/-}$ mice, compared with other groups. (*A*–*F*) WT, $n = 8$; apoE$^{-/-}$, $n = 10$; chronic renal disease apoE$^{-/-}$, $n = 10$. (*G*) Correlation of arterial and valve calcified tissue area (region of interest; pixels). (*H*) Correlation of arterial and valve osteogenic activity (signal intensity; AU). (*G* and *H*) WT, $n = 3$; apoE$^{-/-}$, $n = 4$; chronic renal disease apoE$^{-/-}$, $n = 4$.

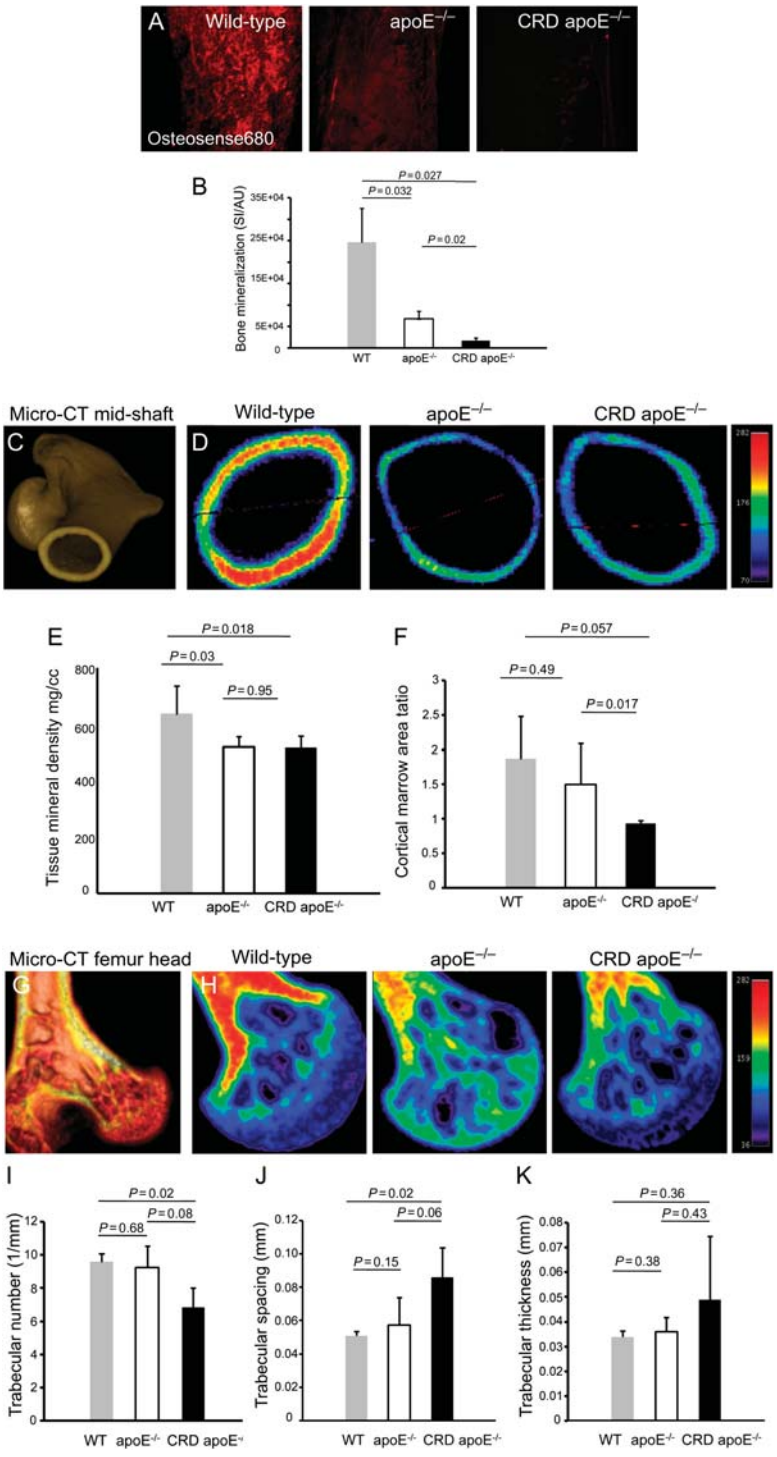

Figure 2 Loss of bone mineral density and alterations in microarchitecture in mouse femurs, detected by 3D micro-computed tomography and molecular imaging. (*A*) Fluorescence microscopy of mid-shaft region of femurs of mice injected with Osteosense680. (*B*) Quantification analysis of bone mineralization signal intensity showed a significant reduction in the chronic renal disease apoE$^{-/-}$ mice, compared with other groups. (*A* and *B*) WT, $n = 8$; apoE$^{-/-}$, $n = 10$; chronic renal disease apoE$^{-/-}$, $n = 10$. (*C* and *D*) Micro-computed tomography imaging of femur mid-shaft region (normal bone = red; loss of bone mineralization = green–blue). (*E*) Quantification assessment of bone tissue mineral density shows significant bone loss in the apoE$^{-/-}$ and chronic renal disease apoE$^{-/-}$ mice. (*F*) Cortical/marrow area shows a tendency towards a decrease in the cortical/marrow ratio in the chronic renal disease apoE$^{-/-}$ mice. (*G* and *H*) Micro-computed tomography imaging of femur head. Quantification assessment of microarchitecture demonstrates (*I*) the decrease in trabecular number and (*J*) the increase in trabecular spacing in the chronic renal disease apoE$^{-/-}$ mice. (*K*) No changes in trabecular thickness were detected. (*C*–*K*) WT, $n = 3$; apoE$^{-/-}$, $n = 4$; chronic renal disease apoE$^{-/-}$, $n = 4$.

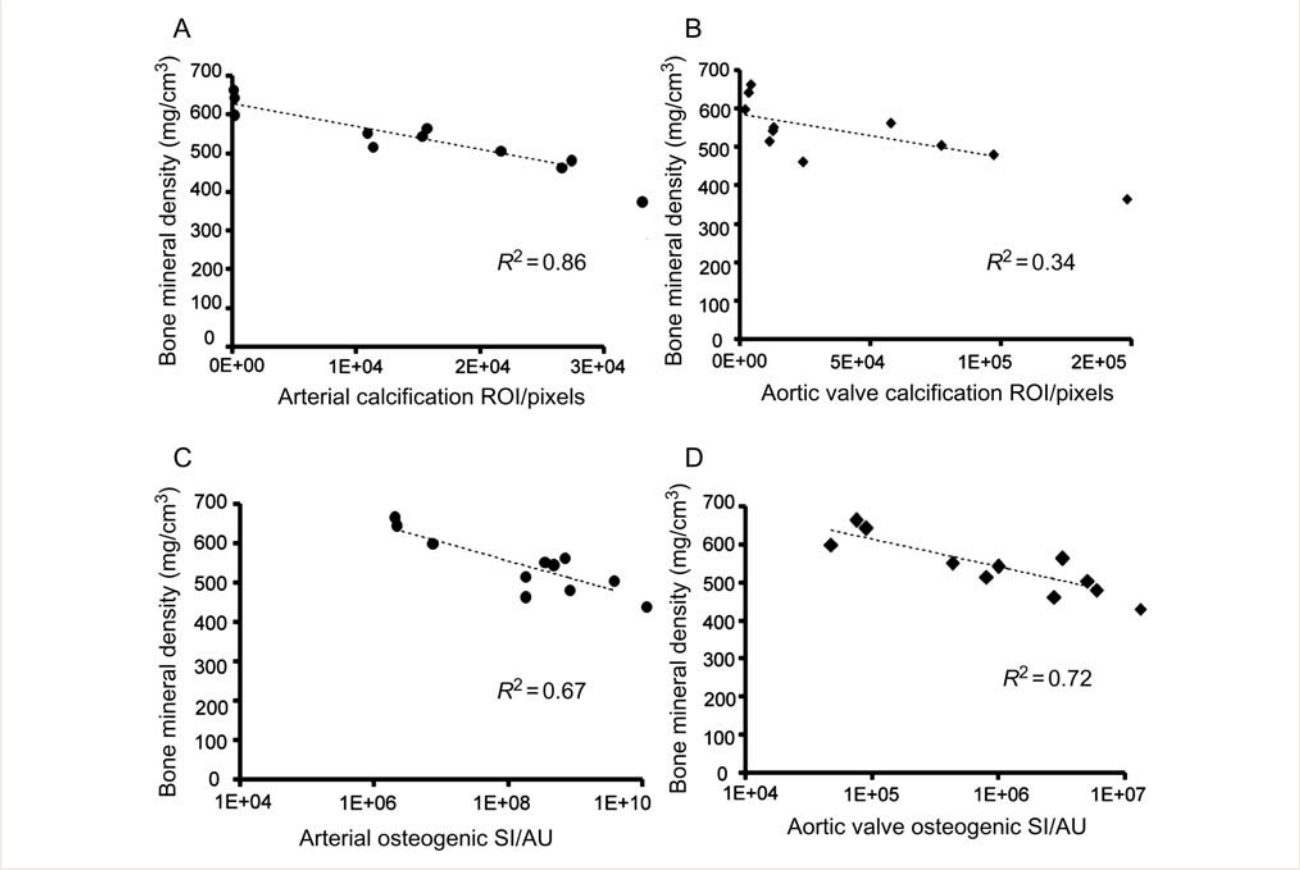

Figure 3 Inverse correlation of bone tissue mineral density with arterial and aortic valve calcification. Relationship of bone tissue mineral density to arterial (*A*) and valve (*B*) calcified area (region of interest). Relationship of tissue mineral density to arterial (*C*) and valve (*D*) osteogenic activity (signal intensity). $n = 11$.

Furthermore, correlative histopathology corroborated our imaging data (Supplementary material online, *Figure S3A* and *B*). These imaging and histological results support the association between arterial and aortic valve calcification.

Bone mineralization decreases in femurs of atherosclerotic mice and inversely correlates to arterial and aortic valve calcification

Figure 2 shows mineralization in the mid-shaft region of femurs in WT, apoE$^{-/-}$, and CRD apoE$^{-/-}$ mice, detected by molecular imaging *ex vivo*. We observed significantly decreased osteogenic SI in apoE$^{-/-}$ mice and CRD apoE$^{-/-}$ mice when compared with WT mice and in apoE$^{-/-}$ mice when compared with CRD apoE$^{-/-}$ mice (*Figure 2A* and *B*). Micro-CT imaging further showed a decrease in bone TMD in the mid-shaft region of femurs from apoE$^{-/-}$ mice when compared with WT mice (*Figure 2C–F*), which supports our molecular imaging results. Quantitative analyses demonstrated a significant difference in TMD between apoE$^{-/-}$ mice and WT mice and between CRD apoE$^{-/-}$ mice and WT mice (*Figure 2E*). Albeit not significant ($P = 0.057$), the difference between CRD apoE$^{-/-}$ mice and WT mice showed a tendency towards decreased cortical/marrow area ratio in CRD apoE$^{-/-}$ mice, suggesting more severe loss of bone structure in the CRD cohort (*Figure 2F*). Periosteal perimeters were not different between conditions, suggesting that the endosteal dimensions expanded through osteoclast activity. Micro-CT showed a decrease in TMD in the femur heads of apoE$^{-/-}$ mice when compared with WT mice (*Figure 2G* and *H*), though bone volume fraction was not significantly changed (Supplementary material online, *Figure S4*). Further statistical analyses of trabecular microarchitecture showed a significant decrease in trabecular number (*Figure 2I*) and a significant increase in trabecular spacing (*Figure 2J*) between CRD apoE$^{-/-}$ mice and WT mice, but there was no significant difference in trabecular thickness between groups (*Figure 2K*). These results suggest that osteoporotic remodelling may occur as a consequence of calcific cardiovascular disease. To test this, we applied a linear regression analysis comparing arterial and valvular calcification with bone TMD (*Figure 3*). Tissue mineral density inversely correlates with the arterial and aortic valve regions of calcification (ROI: $R^2 = 0.86$ and 0.34; respectively; *Figure 3A* and *B*). Furthermore, TMD is inversely correlated to osteogenic SI in carotid arteries and aortic valves (SI: $R^2 = 0.67$ and 0.72, respectively; *Figure 3C* and *D*). These data

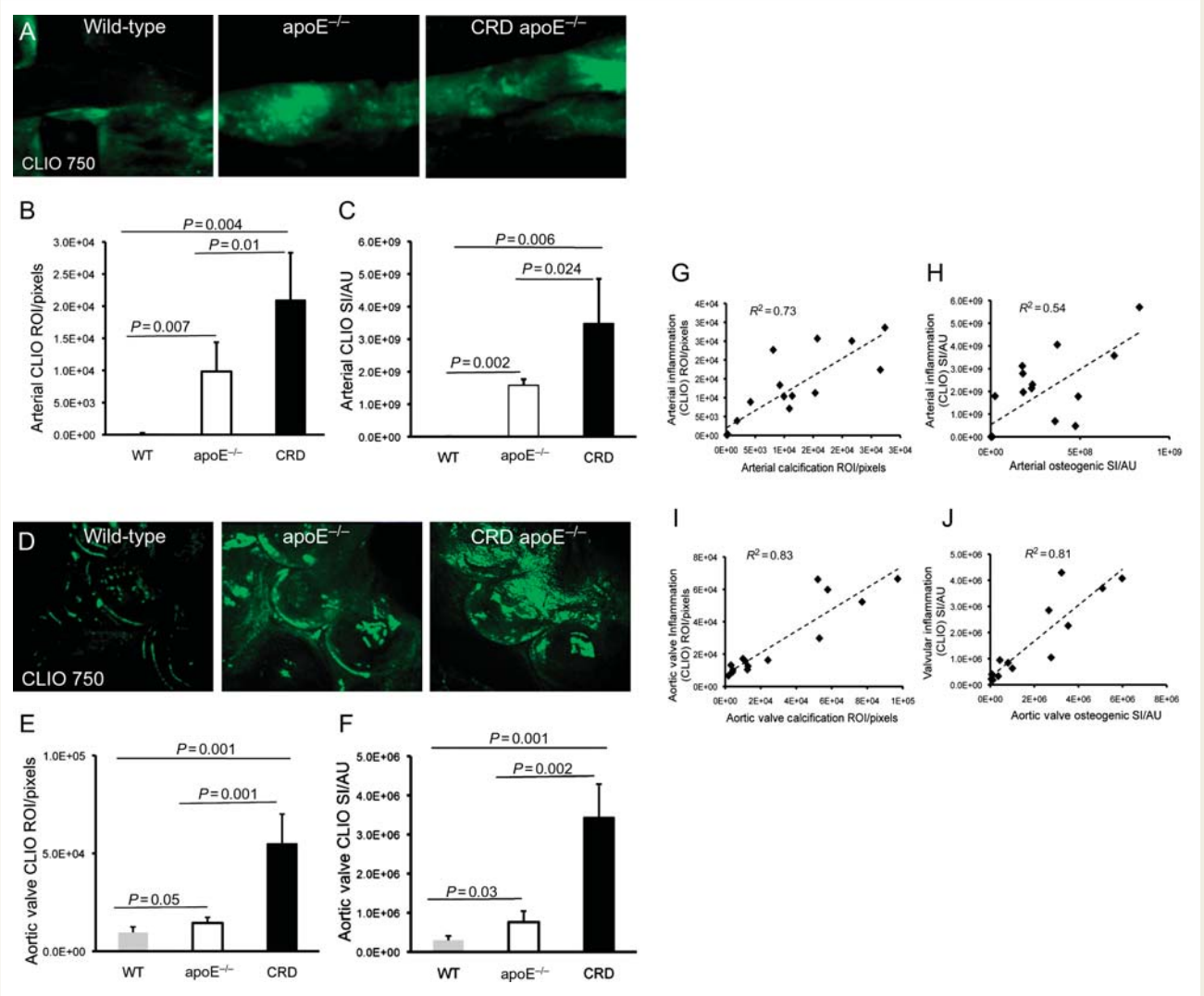

Figure 4 Induction of inflammatory signal in carotid arteries and aortic valves of apoE$^{-/-}$ and chronic renal disease apoE$^{-/-}$ mice, detected by intravital fluorescence microscopy. (*A*) Intravital microscopy detected CLIO750-derived inflammatory signals in the carotid arteries of mice. (*B*) Significant increase in arterial inflammation area (region of interest) and (*C*) inflammatory signal intensity in the chronic renal disease apoE$^{-/-}$ mice vs. WT and apoE$^{-/-}$ mice. (*D*) Fluorescence microscopy detected CLIO750-derived inflammatory signals in the aortic valves. (*E*) Significant increase in the aortic valve inflammation area (region of interest) and (*F*) signal (signal intensity) in the chronic renal disease apoE$^{-/-}$ mice, compared with WT and apoE$^{-/-}$ mice. (*A*–*F*) WT, $n = 8$; apoE$^{-/-}$, $n = 10$; chronic renal disease apoE$^{-/-}$, $n = 10$. (*G*) Relationship between arterial inflammation area (CLIO750; region of interest) and arterial calcified tissue area (Osteosense680; region of interest). (*H*) Association of arterial inflammatory activity (CLIO750; signal intensity) with arterial osteogenic activity (Osteosense680; signal intensity). (*I*) Relationship between valvular inflammation (CLIO750; region of interest) and aortic valve calcification (Osteosense680; region of interest). (*J*) Association of valvular inflammatory signal (CLIO750; signal intensity) with valvular osteogenic activity (Osteosense680; signal intensity). (*G*–*J*) $n = 14$.

suggest a strong inverse correlation between cardiovascular calcification and bone mineralization.

Enhanced inflammation correlates with calcification in arteries and aortic valves

Macrophage-targeted molecular imaging agent (CLIO750) showed negligible inflammatory signal in WT arteries, which was substantially increased in apoE$^{-/-}$ and CRD apoE$^{-/-}$ mice (*Figure 4A*). Quantitative assessment of arterial inflammatory ROI determined a 44- and 95-fold increases in inflammation tissue area in apoE$^{-/-}$ mice and CRD apoE$^{-/-}$ mice when compared with WT mice, which was further confirmed with significant 326- and 718-fold increases in SI (*Figure 4B* and *C*). Likewise, the enhanced expression of inflammation was found in the aortic valves of apoE$^{-/-}$ and CRD apoE$^{-/-}$ mice (*Figure 4D*). Quantitative analyses demonstrated statistically significant increases in inflammatory valvular ROI and SI between WT, apoE$^{-/-}$, and CRD apoE$^{-/-}$

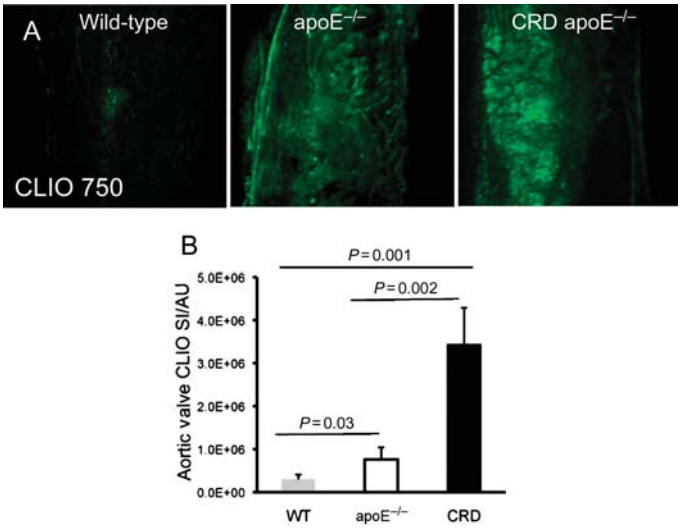

Figure 5 Correlation of long bone inflammation with osteogenic activity. (*A*) Molecular imaging of inflammation in the long bones of mice injected with CLIO750. (*B*) Significant increase in bone inflammation in the chronic renal disease apoE$^{-/-}$ mice vs. WT and apoE$^{-/-}$ mice. (*A* and *B*) WT, $n = 8$; apoE$^{-/-}$, $n = 10$; chronic renal disease apoE$^{-/-}$, $n = 10$.

groups (ROI: 1.5- and 5.7-fold increases, *Figure 4E*; SI: 2.6- and 11.6-fold increases, *Figure 4F*). Further, we found a statistically significant correlation between cardiovascular calcification and inflammation in both arteries (ROI: $R^2 = 0.73$; SI: $R^2 = 0.54$; *Figure 4G* and *H*) and valves (ROI: $R^2 = 0.84$; SI: $R^2 = 0.81$; *Figure 4I* and *J*). Macrophage staining confirmed our molecular imaging findings (Supplementary material online, *Figure S5A* and *B*). Overall, these results suggest that the extent of cardiovascular inflammation correlates with the severity of calcification.

Long bone inflammation correlates inversely with decreased bone mineral signal and associates positively with cardiovascular calcification

Evidence suggests that inflamed or infected bones shift towards an osteolytic environment. To address further the mechanisms for osteoporotic changes, we attempted to link inflammation and TMD in the same mice used for imaging of cardiovascular calcification. Molecular imaging demonstrated robust inflammation signal in the long bones of both apoE$^{-/-}$ mice and CRD apoE$^{-/-}$ mice, whereas WT mice demonstrated virtually no inflammation (*Figure 5A*). Using the same approach as before, we found 7.6- and 22-fold increases in long bone inflammation (CLIO SI) for apoE$^{-/-}$ mice and CRD apoE$^{-/-}$ mice, when compared with WT mice (*Figure 5B*). In contrast to the cardiovascular condition, this increased inflammation correlated with decreased bone mineral signal ($R^2 = 0.75$; *Figure 6A*). These results strongly suggest that the inflammatory responses in long bones contribute to loss of bone mineralization. Finally, we found strong positive correlations in SI between the degree of arterial or valvular inflammation and bone inflammation ($R^2 = 0.97$; *Figure 6B* and *C*). These results support our hypothesis that systemic inflammatory signal simultaneously acts to decrease bone mass and increase cardiovascular calcification.

Discussion

This study establishes direct *in vivo* evidence that the calcification of arteries and aortic valves in atherosclerosis and CRD correlates inversely with bone tissue mineralization. We demonstrate an association between aortic valve calcification and arterial calcification and that the degree of cardiovascular calcification correlates directly with the loss of bone mineral. The increased inflammatory activity in arteries, aortic valves, and long bones in atherosclerosis and renal failure demonstrate that inflammation at these three locations is related probably via systemic or circulating inflammatory cues. Furthermore, our study reveals that whereas macrophage burden positively correlates with the extent of early cardiovascular calcification, inflammation inversely associates with bone mineralization. These results build on previous studies of the pathogenesis of cardiovascular calcification, in which advanced molecular imaging approaches demonstrated that atherosclerotic and aortic valve calcification share similar risk factors and are induced by similar pro-inflammatory molecular and cellular processes.[14–16] Our seemingly paradoxical *in vivo* evidence on inflammation and bone mineralization concur well with previous reports on osteolytic environment in inflamed bones.[24]

Arterial calcification occurs in two different forms: intimal calcification, typically associated with atherosclerosis, and medial calcification, an ossification process associated with renal failure and diabetes.[9] In dysmetabolic patient populations, both types of arterial calcification often develop simultaneously. Intimal calcification increases the risk of plaque rupture, whereas medial calcification increases arterial stiffness and impairs cardiovascular haemodynamics.[9] Although the mechanism remains incompletely

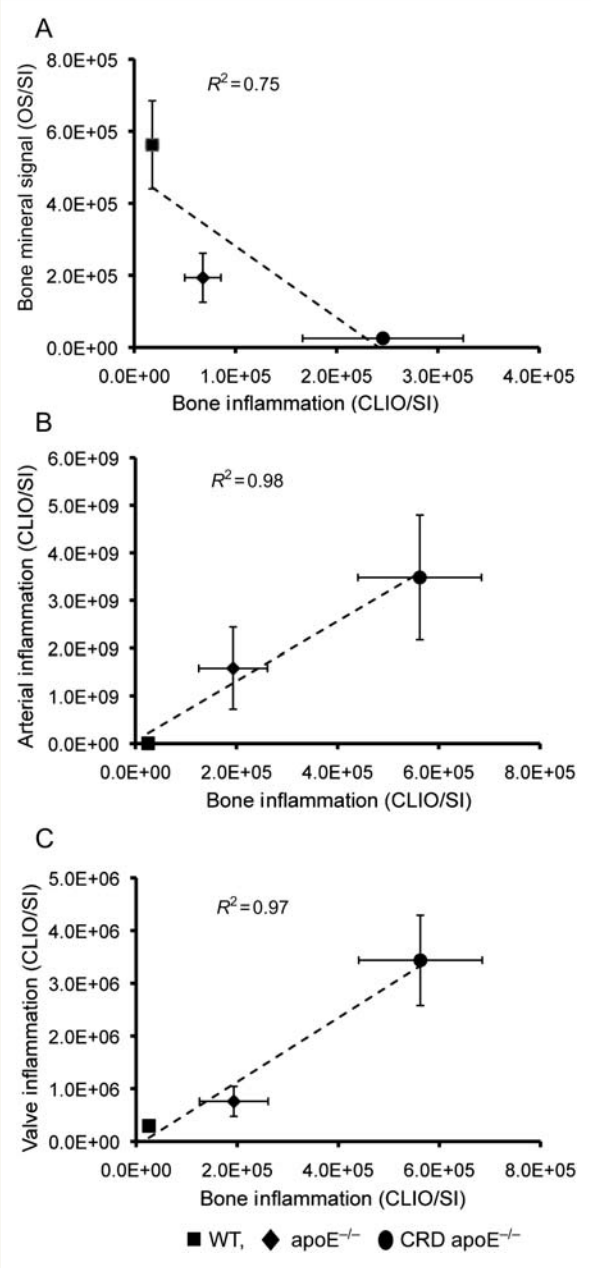

Figure 6 Relationship between bone osteogenic activity and inflammation. (*A*) Inverse association of bone osteogenic activity (Osteosense680; signal intensity) with bone inflammation (CLIO750; signal intensity). (*B*) Positive relationship between arterial inflammation (CLIO750; signal intensity) and bone inflammation (CLIO750; signal intensity). (*C*) Positive correlation of aortic valve inflammation (CLIO750; signal intensity) and bone inflammation (CLIO750; signal intensity). (*A–C*) WT, $n = 8$; apoE$^{-/-}$, $n = 10$; chronic renal disease apoE$^{-/-}$, $n = 10$.

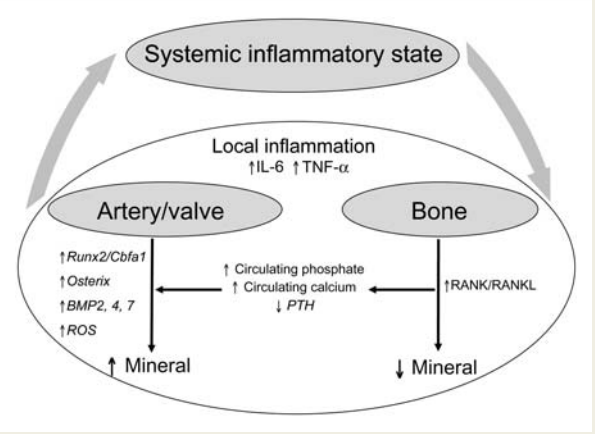

Figure 7 Schematic presentation of a hypothetical model on the paradoxical relationship between cardiovascular calcification and bone mineral loss, associated with local and systemic inflammation. Atherosclerosis and chronic renal disease-associated systemic inflammatory stimuli enhance local inflammation in the cardiovascular system. Local pro-inflammatory microenvironmental cues in atherosclerotic plaques and diseased valves may shift vascular and valvular cells towards an osteogenic phenotype, resulting in increased mineral deposition. In the bone, the inflammatory milieu may increase the number/activity of bone-resorbing osteoclasts, leading to decreased mineral. Additional factors arising from bone could further influence cardiovascular calcification.

understood, it is generally agreed that cardiovascular calcification is a more active biological process than previously considered.[26] Clinicopathological studies have shown similarity between calcified vascular material and bone material,[20] have observed osteoblasts and osteoclast-like cells in the arterial wall,[19] and have demonstrated the presence of various bone-regulating proteins in calcified arteries.[27] Osteogenic differentiation of vascular SMC or valvular myofibroblasts is likely caused by various mechanisms, including pro-inflammatory cytokines (e.g. IL-6, TNF-α),[10] oxidized lipids,[17] and microenvironmental and mechanical cues.[28] Biochemical imbalances also accelerate calcification. Studies show that excess phosphate levels in CRD accelerate calcification of vascular SMC or valvular myofibroblasts through the phosphate-induced release of matrix vesicles and apoptosis.[15,29]

Systemic factors associated with CRD, including reduced circulating levels of erythropoietin, have been shown to reduce osteoblast quantity and bone mineral density via Jak-Stat signalling in haematopoietic stem cells.[30] Furthermore, the kidneys represent the site of vitamin D activation, and therefore CRD-associated reductions in activated vitamin D may also induce parallel reductions in bone mass. Whether CRD-induced anaemia or activated vitamin D deficiency plays a role in the reduced bone mass or increased cardiovascular calcification remains uncertain.

Our results directly quantified a paradox of simultaneous osteolysis and ectopic calcification *in vivo* in the same animals. Although both correlate with age in humans, some clinical studies have shown the association of cardiovascular calcification and osteoporosis to be independent of age.[3,31] Research has demonstrated that patients with lower bone density and osteoporosis have more severe atherosclerosis.[32,33] Dyslipidaemia also may link bone loss with cardiovascular calcification. Pre-clinical studies suggest that hyperlipidaemia reduces bone mineral density[34] and promotes arterial and valvular calcification in mice[14,16] and that

statins reduce calcification.[14,35] Moreover, loss of bone mass leads to increased circulating phosphate and calcium and decreased parathyroid hormone, which stimulate the Cbfa1-dependent mineralization of cardiovascular tissue.[36] This evidence suggests that osteoporosis may contribute to cardiovascular calcification by adding to a pathological microenvironment that promotes osteogenesis of the arterial wall and aortic valve. During bone resorption, biochemical factors are released into the circulation, contributing to vascular calcification; this observation agrees with studies showing that agents that block bone resorption in animal models also block vascular calcification.[37]

Our findings strongly suggest *in vivo* that systemic and local inflammation drives both cardiovascular calcification and bone loss. In general, inflammation causes 'hardening' of soft tissue and 'softening' of hard tissue,[34] but it is unclear whether the pathways are similar. Connections between inflammation and osteolysis were recently established in arthritic and periodontal diseases.[24] Pro-inflammatory cytokines such as IL-6 and TNF-α have been shown to increase the osteoclast activity through the NF-κB pathway.[38] Osteoprotegerin, normally produced by vascular SMC and osteoblasts, functions as a decoy receptor for the receptor activator of NF-κB ligand RANKL.[26] RANKL, a cytokine that induces osteoclast differentiation and activation, stimulates bone resorption, whereas osteoprotegerin neutralizes the binding of RANKL to RANK and prevents bone loss. Osteoprotegerin-deficient mice demonstrated severe bone loss in addition to medial calcifications.[39] Taken together, these studies suggest that inflammation in cardiovascular and bone regions acts through the NF-κB–RANKL pathway, but whether this pathway is utilized simultaneously for ectopic calcification and bone loss is unknown.

Figure 7 shows a schematic illustration of our working hypothesis. The presence of atherosclerosis or CRD likely associates with systemic inflammatory signals, as described above. Local inflammation, as detected by macrophage-targeted NIR fluorescence nanoparticles, associates with increased mineral in cardiovascular tissues and decreased mineral in bone, as detected by Osteosense. Potential mediators associated with systemic and local inflammatory processes are shown, as are possible factors arising from bone, which could further influence cardiovascular calcification. Studies are needed to further establish the relationship between cardiovascular calcification and osteoporosis and to dissect the complex mechanisms for reciprocal regulation of these processes.

Unravelling the mechanisms underlying cardiovascular calcification is an important step towards future strategies. Therapeutic agents that selectively increase or inhibit osteogenesis will be much preferred over current systemic approaches such as statin therapy. The identification of high-risk patients at subclinical stages is an equally important task, requiring new imaging modalities or biomarkers targeting calcification.[8] Molecular imaging provides appealing new means to identify early-stage calcifying atherosclerotic plaques and aortic valve lesions and offers a powerful tool in personalized preventive cardiovascular medicine.

Supplementary material

Supplementary material is available at *European Heart Journal* online.

Acknowledgements

The authors would like to thank Dr Masanori Aikawa for critical reading of the manuscript and Sara Karwacki for excellent editorial assistance.

Funding

This study was supported in part by Wijck-Casper-Stam Foundation (J.H.), American Heart Association Scientist Development Grants (0835460N, E.A.; 0830384N, J.B.), NYSTAR CAT Award (J.B., M.R.), Donald W. Reynolds Foundation (R.W., E.A.), Leducq Foundation (07CVD04; E.A., J.B.) and Translational Program of Excellence in Nanotechnology (5-UO1-HL080731; R.W.). Funding to pay the Open Access publication charges for this article was provided by research grants to Dr Aikawa.

Conflict of interest: R.W. reports serving as a consultant for Visen Medical. Other authors report no disclosures.

References

1. Banks LM, Lees B, MacSweeney JE, Stevenson JC. Effect of degenerative spinal and aortic calcification on bone density measurements in post-menopausal women: links between osteoporosis and cardiovascular disease? *Eur J Clin Invest* 1994;**24**:813–817.
2. Stehman-Breen C. Osteoporosis and chronic kidney disease. *Semin Nephrol* 2004;**24**:78–81.
3. Farhat GN, Cauley JA, Matthews KA, Newman AB, Johnston J, Mackey R, Edmundowicz D, Sutton-Tyrrell K. Volumetric BMD and vascular calcification in middle-aged women: the Study of Women's Health Across the Nation. *J Bone Miner Res* 2006;**21**:1839–1846.
4. Farhat GN, Strotmeyer ES, Newman AB, Sutton-Tyrrell K, Bauer DC, Harris T, Johnson KC, Taaffe DR, Cauley JA. Volumetric and areal bone mineral density measures are associated with cardiovascular disease in older men and women: the health, aging, and body composition study. *Calcif Tissue Int* 2006;**79**:102–111.
5. Frost ML, Grella R, Millasseau SC, Jiang BY, Hampson G, Fogelman I, Chowienczyk PJ. Relationship of calcification of atherosclerotic plaque and arterial stiffness to bone mineral density and osteoprotegerin in postmenopausal women referred for osteoporosis screening. *Calcif Tissue Int* 2008;**83**:112–120.
6. Tintut Y, Morony S, Demer LL. Hyperlipidemia promotes osteoclastic potential of bone marrow cells *ex vivo*. *Arterioscler Thromb Vasc Biol* 2004;**24**:e6–e10.
7. Hirasawa H, Tanaka S, Sakai A, Tsutsui M, Shimokawa H, Miyata H, Moriwaki S, Niida S, Ito M, Nakamura T. ApoE gene deficiency enhances the reduction of bone formation induced by a high-fat diet through the stimulation of p53-mediated apoptosis in osteoblastic cells. *J Bone Miner Res* 2007;**22**:1020–1030.
8. Rajamannan NM, Evans F, Aikawa E, Grande-Allen KJ, Heistad DD, Masters KS, Mathieu P, O'Brien K, Otto CM, Schoen FJ, Simmons G, Towler D, Yoganathan A. National Heart, Lung and Blood Institute (NHLBI) Working Group on Calcific Aotic Stenosis. http://www.nhlbi.nih.gov/meetings/workshops/cas.htm. 2010.
9. Wayhs R, Zelinger A, Raggi P. High coronary artery calcium scores pose an extremely elevated risk for hard events. *J Am Coll Cardiol* 2002;**39**:225–230.
10. Abedin M, Tintut Y, Demer LL. Vascular calcification: mechanisms and clinical ramifications. *Arterioscler Thromb Vasc Biol* 2004;**24**:1161–1170.
11. Virmani R, Burke AP, Farb A, Kolodgie FD. Pathology of the vulnerable plaque. *J Am Coll Cardiol* 2006;**47**(Suppl. 8):C13–C18.
12. Vengrenyuk Y, Cardoso L, Weinbaum S. Micro-CT based analysis of a new paradigm for vulnerable plaque rupture: cellular microcalcifications in fibrous caps. *Mol Cell Biomech* 2008;**5**:37–47.
13. Hoshino T, Chow LA, Hsu JJ, Perlowski AA, Abedin M, Tobis J, Tintut Y, Mal AK, Klug WS, Demer LL. Mechanical stress analysis of a rigid inclusion in distensible material: a model of atherosclerotic calcification and plaque vulnerability. *Am J Physiol* 2009;**297**:H802–H810.
14. Aikawa E, Nahrendorf M, Sosnovik D, Lok VM, Jaffer FA, Aikawa M, Weissleder R. Multimodality molecular imaging identifies proteolytic and osteogenic activities in early aortic valve disease. *Circulation* 2007;**115**:377–386.
15. Aikawa E, Aikawa M, Libby P, Figueiredo JL, Rusanescu G, Iwamoto Y, Fukuda D, Kohler RH, Shi GP, Jaffer FA, Weissleder R. Arterial and aortic valve calcification abolished by elastolytic cathepsin S deficiency in chronic renal disease. *Circulation* 2009;**119**:1785–1794.

16. Aikawa E, Nahrendorf M, Figueiredo JL, Swirski FK, Shtatland T, Kohler RH, Jaffer FA, Aikawa M, Weissleder R. Osteogenesis associates with inflammation in early-stage atherosclerosis evaluated by molecular imaging *in vivo*. *Circulation* 2007;**116**:2841–2850.
17. Miller JD, Chu Y, Brooks RM, Richenbacher WE, Pena-Silva R, Heistad DD. Dysregulation of antioxidant mechanisms contributes to increased oxidative stress in calcific aortic valvular stenosis in humans. *J Am Coll Cardiol* 2008;**52**:843–850.
18. Rajamannan NM, Nealis TB, Subramaniam M, Pandya S, Stock SR, Ignatiev CI, Sebo TJ, Rosengart TK, Edwards WD, McCarthy PM, Bonow RO, Spelsberg TC. Calcified rheumatic valve neoangiogenesis is associated with vascular endothelial growth factor expression and osteoblast-like bone formation. *Circulation* 2005;**111**:3296–3301.
19. Bostrom K, Watson KE, Stanford WP, Demer LL. Atherosclerotic calcification: relation to developmental osteogenesis. *Am J Cardiol* 1995;**75**:88B–91B.
20. Duer MJ, Friscic T, Proudfoot D, Reid DG, Schoppet M, Shanahan CM, Skepper JN, Wise ER. Mineral surface in calcified plaque is like that of bone: further evidence for regulated mineralization. *Arterioscler Thromb Vasc Biol* 2008;**28**:2030–2034.
21. Rabkin E, Aikawa M, Stone JR, Fukumoto Y, Libby P, Schoen FJ. Activated interstitial myofibroblasts express catabolic enzymes and mediate matrix remodeling in myxomatous heart valves. *Circulation* 2001;**104**:2525–2532.
22. Rattazzi M, Bennett BJ, Bea F, Kirk EA, Ricks JL, Speer M, Schwartz SM, Giachelli CM, Rosenfeld ME. Calcification of advanced atherosclerotic lesions in the innominate arteries of ApoE-deficient mice: potential role of chondrocyte-like cells. *Arterioscler Thromb Vasc Biol* 2005;**25**:1420–1425.
23. Steitz SA, Speer MY, Curinga G, Yang HY, Haynes P, Aebersold R, Schinke T, Karsenty G, Giachelli CM. Smooth muscle cell phenotypic transition associated with calcification: upregulation of Cbfa1 and downregulation of smooth muscle lineage markers. *Circ Res* 2001;**89**:1147–1154.
24. Lerner UH. Inflammation-induced bone remodeling in periodontal disease and the influence of post-menopausal osteoporosis. *J Dent Res* 2006;**85**:596–607.
25. Kozloff KM, Volakis LI, Marini JC, Caird MS. Near-infrared fluorescent probe traces bisphosphonate delivery and retention *in vivo*. *J Bone Miner Res*; doi:10.1002/jbmr.66. Published online ahead of print 2010.
26. Demer LL, Tintut Y. Vascular calcification: pathobiology of a multifaceted disease. *Circulation* 2008;**117**:2938–2948.
27. El-Abbadi M, Giachelli CM. Mechanisms of vascular calcification. *Adv Chronic Kidney Dis* 2007;**14**:54–66.
28. Yip CY, Chen JH, Zhao R, Simmons CA. Calcification by valve interstitial cells is regulated by the stiffness of the extracellular matrix. *Arterioscler Thromb Vasc Biol* 2009;**29**:936–942.
29. Reynolds JL, Joannides AJ, Skepper JN, McNair R, Schurgers LJ, Proudfoot D, Jahnen-Dechent W, Weissberg PL, Shanahan CM. Human vascular smooth muscle cells undergo vesicle-mediated calcification in response to changes in extracellular calcium and phosphate concentrations: a potential mechanism for accelerated vascular calcification in ESRD. *J Am Soc Nephrol* 2004;**15**:2857–2867.
30. Shiozawa Y, Jung Y, Ziegler AM, Pedersen EA, Wang J, Wang Z, Song J, Wang J, Lee CH, Sud S, Pienta KJ, Krebsbach PH, Taichman RS. Erythropoietin couples hematopoiesis with bone formation. *PLoS ONE* **5**:e10853.
31. Hak AE, Pols HA, van Hemert AM, Hofman A, Witteman JC. Progression of aortic calcification is associated with metacarpal bone loss during menopause: a population-based longitudinal study. *Arterioscler Thromb Vasc Biol* 2000;**20**:1926–1931.
32. Browner WS, Seeley DG, Vogt TM, Cummings SR. Non-trauma mortality in elderly women with low bone mineral density. Study of Osteoporotic Fractures Research Group. *Lancet* 1991;**338**:355–358.
33. Uyama O, Yoshimoto Y, Yamamoto Y, Kawai A. Bone changes and carotid atherosclerosis in postmenopausal women. *Stroke* 1997;**28**:1730–1732.
34. Demer LL. Vascular calcification and osteoporosis: inflammatory responses to oxidized lipids. *Int J Epidemiol* 2002;**31**:737–741.
35. Rajamannan NM, Subramaniam M, Springett M, Sebo TC, Niekrasz M, McConnell JP, Singh RJ, Stone NJ, Bonow RO, Spelsberg TC. Atorvastatin inhibits hypercholesterolemia-induced cellular proliferation and bone matrix production in the rabbit aortic valve. *Circulation* 2002;**105**:2660–2665.
36. Jono S, Nishizawa Y, Shioi A, Morii H. 1,25-Dihydroxyvitamin D3 increases *in vitro* vascular calcification by modulating secretion of endogenous parathyroid hormone-related peptide. *Circulation* 1998;**98**:1302–1306.
37. Price PA, June HH, Buckley JR, Williamson MK. Osteoprotegerin inhibits artery calcification induced by warfarin and by vitamin D. *Arterioscler Thromb Vasc Biol* 2001;**21**:1610–1616.
38. Crotti TN, Smith MD, Findlay DM, Zreiqat H, Ahern MJ, Weedon H, Hatzinikolous G, Capone M, Holding C, Haynes DR. Factors regulating osteoclast formation in human tissues adjacent to peri-implant bone loss: expression of receptor activator NFkappaB, RANK ligand and osteoprotegerin. *Biomaterials* 2004;**25**:565–573.
39. Bucay N, Sarosi I, Dunstan CR, Morony S, Tarpley J, Capparelli C, Scully S, Tan HL, Xu W, Lacey DL, Boyle WJ, Simonet WS. Osteoprotegerin-deficient mice develop early onset osteoporosis and arterial calcification. *Genes Dev* 1998;**12**:1260–1268.